Stapp Car Crash Journal 44 (November 2000) 205-213

2000-01-SC15

Defining Brain Mechanical Properties: Effects of Region, Direction, and Species

Michael T. Prange, David F. Meaney, Susan S. Margulies
University of Pennsylvania

ABSTRACT

No regional or directional large-deformation constitutive data for brain exist in the current literature. To address this deficiency, the large strain (up to 50%) directional properties of gray and white matter were determined in the thalamus, corona radiata, and corpus callosum. The constitutive relationships of all regions and directions are well fit by an Ogden hyperelastic relationship, modified to include dissipation. The material parameter α, representing the non-linearity of the tissue, was not significantly sensitive to region, direction, or species. The average value of the material parameter μ, corresponding to the shear modulus of the tissue, was significantly different for each region, demonstrating that brain tissue is inhomogeneous. In each region, μ, obtained in 2 orthogonal directions, was compared. Consistent with local neuroarchitecture, gray matter showed the least amount of anisotropy and corpus callosum exhibited the greatest degree of anisotropy. Finally, human temporal lobe gray matter properties were determined and compared to porcine thalamic properties. The results show significant regional inhomogeneity at large strains and significant anisotropy in each region tested. The extent of regional anisotropy correlated with the degree of alignment in the local neuroarchitecture. These large strain, regional and directional data should enhance the biofidelity of computational models and provide important information regarding the mechanisms of traumatic brain injury.

INTRODUCTION

Biomechanical analyses of diffuse axonal injury (DAI) suggest a link between brain material response (strain) and white matter injury [1-6]. Material properties of the brain tissue, including a description of their inhomogeneity, are important to predict intracranial deformations from the applied inertial loads. It is essential that these properties are defined separately for the gray and white matter and account for the potential nonlinear viscoelastic behavior at finite strains.

Material properties of brain tissue have been measured in vitro during compression, shear, and oscillatory loading [7-17] and the reported properties vary by as much as an order of magnitude. This range is probably related to the anisotropic and inhomogeneous nature of brain tissue and the broad range of test conditions.

White matter consists of a fiber arrangement that is highly oriented, while gray matter consists of cell bodies and supporting vascular network that likely do not impose such directional preference. Magnetic resonance diffusion tensor images of the brain neuroarchitecture confirm that some regions of white matter can be modeled as transversely isotropic, while gray matter is an isotropic structure [18]. Despite this evidence, though, few investigators have examined brain's directional properties. Only Shuck and Advani included brain's anisotropy and inhomogeneity in their study design [16]. Shuck and Advani's important and encouraging data were obtained at very small strains of 1.3%, considerably smaller than those associated with traumatic head injury.

In this paper, we present data defining the regional and directional properties of brain tissue at strains up to 50%. We hypothesized that gray matter has a homogeneous and isotropic tissue structure. Previously we demonstrated that brainstem can be represented by a fiber-reinforced composite where the uniaxially oriented viscoelastic fibers (neural tracts) are three times stiffer than the surrounding viscoelastic matrix (extracellular components and oligodendrocytes) in the brainstem region [19]. Because oriented neural tracts also exist within the cerebral white matter, we hypothesized it would have anisotropic mechanical properties. We also hypothesized that, within the white matter, different degrees of anisotropy would exist depending on the extent of fiber orientation and tested two regions of cerebral white matter, the corpus callosum and corona radiata. The corpus callosum is a uniaxially oriented region of the brain consisting of neural tracts running between the left and right hemispheres. We hypothesized that this region would resemble our previous findings in the brainstem. In contrast, the

corona radiata is also composed of neural tracts, but the tissue is not uniaxially oriented; the fibers appear in a 'fan' pattern along a major axis. Due to this organization, we hypothesized that the corona radiata has a lower degree of anisotropy than corpus callosum.

In summary, the focus of this paper is on a critical gap in the existing literature: identifying the inhomogeneity and anisotropy of brain tissue at large strains. We hypothesized the white matter is anisotropic due to its cellular architecture, while the gray matter would posses much less directional dependence in its material properties.

METHODS

SAMPLE PROCUREMENT AND PREPARATION - To test brain tissue for inhomogeneity and anisotropy, rectangular porcine tissue samples (10 x 5 x 1 mm) were excised from sections of white matter (corona radiata and corpus callosum) and gray matter (thalamus) maintaining consistent orientation from animal to animal. All samples were transported in mock CSF solution and tested within 5 hours postmortem [20]. Specimen dimensions (length, width, thickness) were measured in triplicate with a digital caliper and averaged.

In the gray matter, Direction 1 (D1) was defined as the superior/inferior direction, and Direction 2 (D2) was defined as the transverse direction in the coronal plane (Figure 1a). In corona radiata samples, D1 was defined as aligned with the neural tracts in the coronal plane, and D2 was defined as orthogonal to the tracts in the coronal plane (Figure 1b). In the corpus callosum samples, D1 was defined as aligned with the neural tracts in the transverse plane and D2 was defined as orthogonal to the tracks in the transverse plane (Figure 1c). Each sample was tested along only one direction. We tested 18 corona radiata white matter samples (12 D1, 6 D2), 12 corpus callosum samples (6 D1, 6 D2) and 18 gray matter samples (12 D1, 6 D2) from a total of 32 brains.

Fresh human remnant temporal cortex samples (gray matter, N=5), obtained from the operating suite after temporal lobectomy procedures, were tested within 3 hours after excision. Data were compared with porcine tissue data. All protocols were approved by the University of Pennsylvania IACUC and IRB.

TESTING PROTOCOLS - Using a custom designed, humidified, parallel-plate shear testing device [21], displacement and force were measured during rapid stress relaxation tests in simple shear. The bottom plate was displaced with a ramp time of 60 msec and hold time of 60 sec in the following order of approximate strain (ε_{12}) magnitudes: 2.5%, 5%, 10%, 20%, 30%, 40%, 50%, and retested at 5% to confirm reproducibility. Each specimen was tested at strain rates ranging between 0.42 and 8.33 s^{-1}.

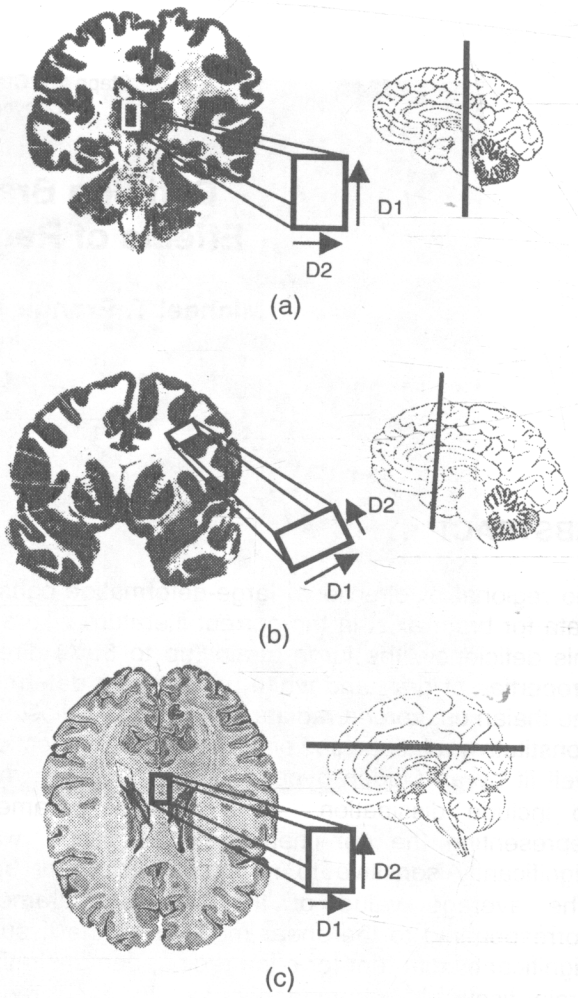

Figure 1: Anatomic locations and test directions (D1= direction 1, D2= direction 2) of (a) gray matter sample and (b) corona radiata sample shown in coronal section (left) and sagittal section (right). Anatomic location of (c) corpus callosum sample shown in transverse section (left) and sagittal section (right).

Data was obtained (1kHz sampling rate) at each strain level after two preconditioning runs at that strain level and stored on computer. For each strain level, force and displacement data at five isochrones (100 msec, 300 msec, 800 msec, 1800 msec, and 60 sec after peak) from each specimen were evaluated to determine the properties for the specified tissue type and direction.

Following the shear testing, unconfined compression experiments were conducted to test the validity of the hyperelastic model in a different testing mode. Gray matter samples (10x 5 x 2.5 mm, n=4) were compressed using a stress relaxation protocol at 5%, 30%, and 50% strain (ε_{22}). The tissue was placed in a parallel plate indentor and the top plate controlled by a stepper motor (Model 26449-05, Haydon Switch and Instrument, Inc., Waterbury, CT). The displacement of the top plate was measured with an LVDT (Model 0241, Trans-Tek, Inc, Ellington, CT) and the resulting compressive force was

measured with an axial force transducer (Model 31, Sensotec, Columbus, OH). The plates were lubricated (Braycote 804 Grease, Castol, Irvine, CA) to ensure a pure slip boundary that was confirmed photographically. The displacement ramp rate was approximately 1.5 mm/sec (strain rate of 0.6 sec^{-1}), followed by a 60sec hold. Data was obtained at each strain level after two preconditioning runs were performed. The measured long-term nominal stress values (t=60sec) were compared to the predictions of the long-term nominal stress generated for unconfined compression using the Ogden hyperelastic model and the parameters determined from the shear tests.

INTERFACIAL TESTING CONDITIONS - Studies were designed to confirm that the shear testing protocol provided a no-slip boundary condition at the two glass plates and was non-destructive to the tissue. The no-slip boundary condition was examined by marking the tissue, displacing the bottom plate 1mm (ε_{12}=50%), and measuring the displacement of the tissue at the top plate from photographs. The tissue was marked with cresyl violet and a 25mm grid secured on the top glass plate. The locations of five points on the tissue were digitized at the top tissue surface relative to the grid and compared to the digitizing error.

TISSUE INTEGRITY ASSESSMENT - To demonstrate that the testing protocol did not damage the tissue, a mixed gray/white matter sample near the corona radiata was subjected to 50% shear strain and compared to an unstrained sample obtained from the same excised brain specimen. Both samples were fixed and microtome sections were stained with a Nissl stain to examine cellular integrity. The cell bodies' size, shape, distribution, organization, and stain intensity were compared.

An additional assessment of the tissue integrity was conducted comparing the final test at 5% shear strain after the entire multi-test protocol was completed. The long-term moduli (G_∞) of the initial and final 5% tests of 12 samples were compared with a paired Student's t test. If the samples were not damaged during the test, we would expect these two test conditions to yield similar results.

ANALYSIS

A strain energy-based constitutive model was developed to describe the behavior of white and gray matter in orthogonal simple shear tests. Isotropy and homogeneity were assumed for each sample tested, and a comparison of properties obtained in different directions was employed to evaluate anisotropy. Future work may incorporate the directional properties into a single anisotropic material model. The nonlinear material properties were modeled with a first order Ogden hyperelastic model modified to include energy dissipation. In this approach, we started with a formulation for an elastic material based on a first order Ogden hyperelastic material with a strain energy density function W [22]:

$$W = \frac{2\mu}{\alpha^2}(\lambda_1^\alpha + \lambda_2^\alpha + \lambda_3^\alpha - 3) \quad (1)$$

where α and μ are properties of the material, and λs are the principal stretch ratios. The parameter α incorporates the strain-magnitude sensitive nonlinear characteristics, and μ corresponds to the shear modulus of the tissue. In simple shear (λ_3 =1), the maximum principal stretch ratio λ is related to the engineering shear strain γ ($2\varepsilon_{12}$) [22]:

$$\lambda = \frac{\gamma}{2} + \sqrt{1 + \frac{\gamma^2}{4}} \quad (2)$$

Assuming incompressibility ($\lambda_1 \cdot \lambda_2 \cdot \lambda_3$=1), the elastic component of the shear stress (T_{12}) measured on top face of the tissue sample is related to the applied shear:

$$T_{12} = \frac{2\mu}{\alpha}\frac{(\lambda^\alpha - \lambda^{-\alpha})}{(\lambda + \lambda^{-1})} \quad (3)$$

To incorporate time dependent behavior, we replaced the shear modulus in the above expression (μ) with a modulus that changes with time, $\mu(t)$. This formulation assumes that α is independent of time and $\mu(t)$ is independent of strain.

To determine the parameter α in our constitutive relationship independently of μ, we examined the isochrone data from our stress relaxation tests. At a fixed stress isochrone ($t=t_i$), we normalized the measured stress response across the seven different strain magnitudes tested to the stress at a specific shear level ($\gamma=\gamma_o$). This yielded the following expression for normalized shear at time t_i that was independent of μ:

$$T_{12,norm}(\lambda, t_i) = \frac{T_{12}(\lambda, t_i)}{T_{12}(\lambda_0, t_i)} = \frac{(\lambda^\alpha - \lambda^{-\alpha})(\lambda_0 + \lambda_0^{-1})}{(\lambda_0^\alpha - \lambda_0^{-\alpha})(\lambda + \lambda^{-1})} \quad (4)$$

where λ_o is the principal stretch at the shear γ_o. Using the definitions above, we calculated the T_{12}, γ, and λ values at each isochrone from the force and displacement data recorded from all ramp-and-hold stress relaxation experiments and normalized the values to γ_o=0.50 (ε_{12}=25%). The stress at 25% strain was determined by interpolating between the stress measured at the 20% and 30% shear strain tests. To determine α for the first order Ogden model, all isochrone and strain data for a particular tissue and test direction was combined and fit to Equation 4 using a least-squares nonlinear regression (IGOR Pro 3.1.4, Wavemetrics, Lake Oswego, OR). To confirm that the overall α value was time-independent, we evaluated Equation 4 at each isochrone as well.

Once α was determined, we re-analyzed the measured relaxation response at each isochrone to determine the relaxation modulus $\mu(t)$. Using the overall α determined for that tissue type and direction, we rearranged Equation 3 to solve for μ at each isochrone to calculate the shear relaxation modulus $\mu(t_i)$ directly at each of these times t_i.

$$\mu_i(t_i) = \frac{\alpha T_{12}(\lambda + \lambda^{-1})}{2(\lambda^{\alpha} - \lambda^{-\alpha})} \quad (5)$$

To determine μ at a specific isochrone, all strain data of all samples for a particular tissue region and test direction at that time point was combined and fit to Equation 5 using least-squares linear regression. The data at each isochrone were combined into a single second order Prony series for a particular region and test direction:

$$\mu(t) = \mu_0\left(1 - \sum_{i=1}^{2} C_i\left(1 - e^{-t/\tau_i}\right)\right) \quad (6)$$

To confirm that $\mu(t)$ was independent of λ, we evaluated data at individual strain levels used to fit to Equation 5. Student's *t* analyses for comparing two slopes were performed on $\mu(t)$ at each time point to determine any significant differences between the corona radiata, corpus callosum, human temporal cortex or gray matter properties and whether, within a tissue type, properties in Direction 1 were significantly different from those in Direction 2.

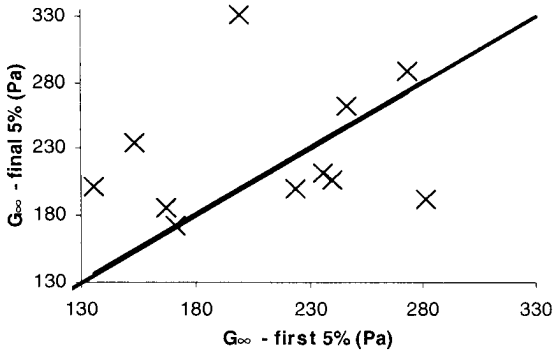

Figure 2: Long-term shear moduli of first and final 5% shear strain tests. (line has slope=1)

RESULTS

INTERFACIAL TESTING CONDITIONS - The no-slip boundary condition for the shear testing mode was confirmed with the analysis of displacement of the tissue at the top plate during the largest tissue strain (ε_{12}=50%). The five points digitized had an average displacement of 0.009mm with a digitizing error of 0.008mm. The tissue displacement was statistically indistinguishable from the digitizing error and was less than 1% of the displacement of the bottom plate.

The pure slip condition between the plates and tissue in the unconfined compression tests was evaluated photographically. Given a bulk modulus of approximately 2 MPa (300,000 psi) [23], we assumed that brain tissue was incompressible. The change in surface area of the tissue samples, evaluated at 50% compression, differed less than 1% from that predicted for an incompressible material, confirming the pure slip boundary at the plates for this testing mode.

TISSUE INTEGRITY ASSESSMENT - The Nissl staining revealed no difference between the unstrained tissue and tissue strained with the 50% shear strain protocol. The cell bodies had similar size, shape, distribution, organization, and stain intensity, indicating no tissue discernable damage as a result of the testing protocol.

Figure 2 shows an identity plot of G_∞ of the first and final 5% shear strain test for each sample. The plot shows no consistent pattern between the first and final shear modulus. Tissue damage for the shear testing mode was also verified after a sample was subjected to 50% shear strain. Paired –t analysis of the long-term moduli (G_∞) of the first and final 5% (ε_{12}) shear strain were not significantly different (p=0.33, n=12), demonstrating the testing protocol did not alter the tissue.

SHEAR MATERIAL PROPERTIES - We determined there was no consistent influence of time on the Equation 4 relationship nor of strain on the Equation 5 relationship, confirming that the response of gray matter and white matter samples tested in a single direction could be represented using this modified hyperelastic material model. The parameters for each tissue type and direction are shown in Table 1.

The coefficient of determination (R^2) was ≥87% for each fit to Equation 4, supporting the Ogden model as an appropriate material model to represent the nonlinearity of brain tissue (Figure 3). The α value was varied for each tissue region and direction to determine the sensitivity of the curve fit to the α value. The R^2 value changed less than 1% when α was varied by an order of magnitude (0.002–0.8). Therefore, given the relatively narrow range of α values reported in Table 1 (0.0273 – 0.0759), we conclude that values of α did not vary significantly across either tissue type or direction.

Table1: Ogden coefficients α and $\mu(t)$ (2^{nd} order Prony series, Eqn 6) for all regions, directions and species

Species	Human	Porcine								
Region	Gray	Gray Matter (thalamus)			Corona Radiata			Corpus Callosum		
Direction		D1	D2	avg	D1	D2	avg	D1	D2	avg
# samples	5	12	6	18	12	6	18	6	6	12
α	0.0323	0.0273	0.0600	0.0382	0.0741	0.0360	0.0614	0.0497	0.0759	0.0628
μ_0 (Pa)	295.7	271.5	256.1	263.6	292.6	211.4	254.2	131.4	232.2	182.2
C_1	0.335	0.302	0.296	0.300	0.288	0.265	0.279	0.297	0.264	0.276
τ_1 (sec)	2.40	2.71	2.49	2.60	2.86	2.42	2.72	2.590	3.03	2.85
C_2	0.461	0.451	0.478	0.464	0.497	0.516	0.505	0.474	0.462	0.466
τ_2 (sec)	0.146	0.186	0.165	0.175	0.167	0.167	0.166	0.151	0.162	0.158

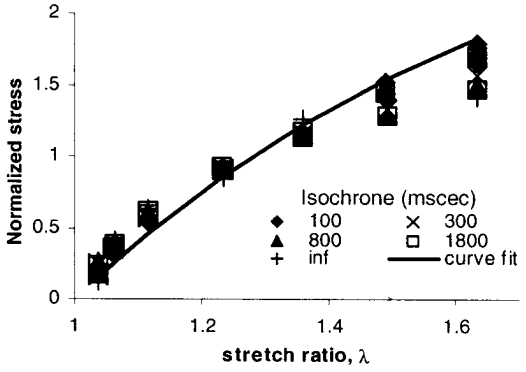

Figure 3: Typical non-linear regression to determine the constant α. Data shown for 1 sample.

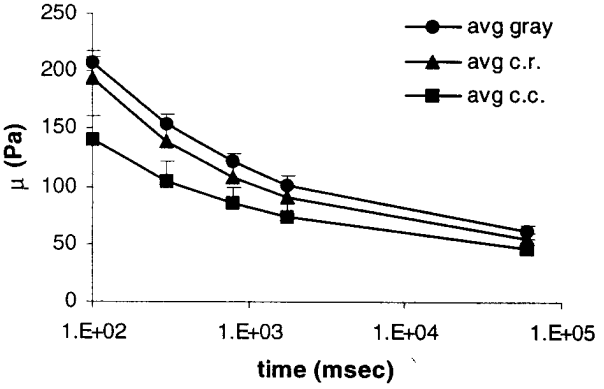

Figure 5: Regional properties. Time dependent Ogden component μ for corona radiata (c.r.), corpus callosum (c.c.) and gray matter (error bars indicate 95% confidence interval)

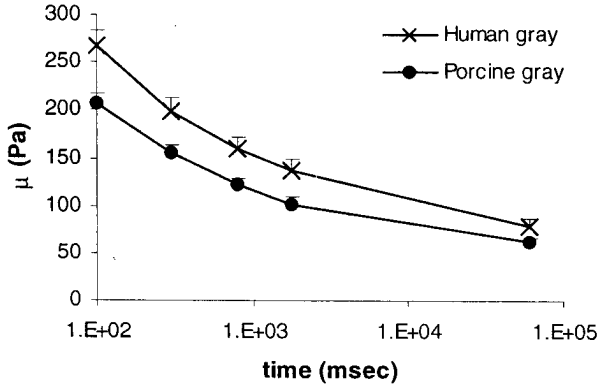

Figure 4: Time dependent Ogden parameter μ for human and porcine gray matter (error bars indicate 95% confidence interval)

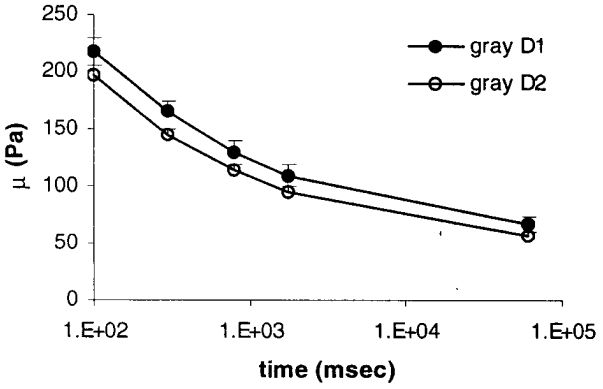

Figure 6: Directional properties. Time dependent Ogden component μ for gray matter (error bars indicate 95% confidence interval)

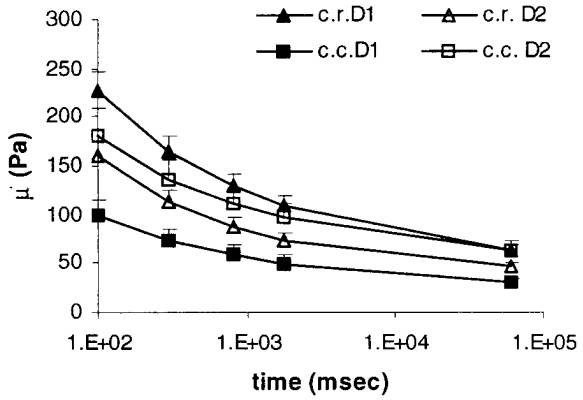

Figure 7: Directional properties. Time dependent Ogden component μ for white matter regions corona radiata (c.r.) and corpus callosum (c.c.) (error bars indicate 95% confidence interval)

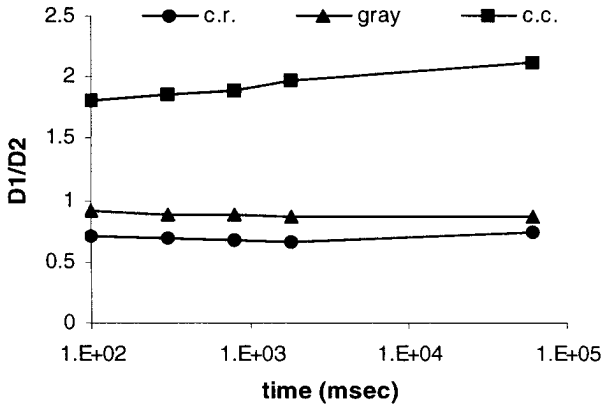

Figure 8: Directional properties. Direction ratio (D1/D2) or gray matter, corona radiata (c.r.) and corpus callosum (c.c.)

To compare human and porcine properties, a mean porcine gray matter μ(t) was computed from the average D1 and D2 properties at each isochrone. At each isochrone, μ(t) was significantly different between human gray matter (n=5) and porcine gray matter (n=18) ($p<0.001$, Figure 4). The human samples were an average of 29% (37.7 Pa) stiffer than the porcine samples.

To evaluate regional inhomogeneity, a mean μ(t) was calculated from the average D1 and D2 at each isochrone (Figure 5). Each tissue region was significantly different from the others at every time point ($p<0.05$). Gray matter had the largest average μ while corpus callosum had the lowest average μ at every time point.

To evaluate intra-regional anisotropy, comparisons were made between D1 and D2 results obtained from each region. Directions 1 and 2 for each tissue type all were significantly different ($p<0.05$), but only corpus callosum had D2 properties greater that D1 (Figure 6,7). The ratio (D2/D1) of μ was evaluated at each time point and averaged to yield approximately 0.88, 0.70 and 1.93 for

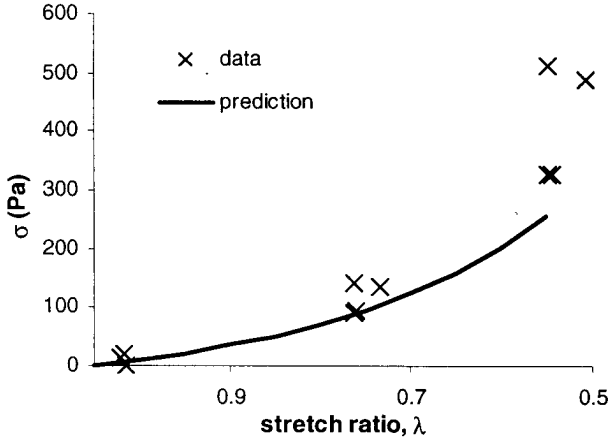

Figure 9: Long term stress of unconfined compression experiments compared to prediction of Ogden material model.

gray matter, corona radiata and corpus callosum respectively (Figure 8).

To evaluate directional properties across regions, comparisons were made between the corona radiata and corpus callosum results obtained from the same direction. Corona radiata was significantly ($p<0.001$) stiffer than corpus callosum for D1 (parallel to fiber direction) at all time points. Direction 2 properties were statistically indistinguishable between the two white matter regions at the first two isochrones, but were significantly different at the 800msec, 1800msec and 60sec isochrones (Figure 7).

Taken together, these findings from the porcine shear tests support our hypotheses that white matter and gray matter have distinct properties, and that white matter behavior is more anisotropic than gray matter. These findings also support our hypotheses that different degrees of anisotropy exist within the white matter, a finding that we propose correlates with the neurostructural organization in these regions.

VALIDATION IN UNCONFINED COMPRESSION – Results for unconfined compression of porcine gray matter samples showed a typical relaxation response to the ramp and hold compression. The measured long-term stress values from the gray matter compression experiments conducted are shown in Figure 9. Using the average material parameters describing the shear properties of gray matter, these measured compression results were compared to the predictions of the Ogden hyperelastic model. The results show excellent agreement, with a R^2 value of 84% for the prediction, thus validating this material model in a second independent test mode.

DISCUSSION

This extensive determination of the mechanical properties of brain tissue at large strains, including the effects of region, direction and species, represents a major step forward in our understanding of the response

of the brain during traumatic events. As such, it is important to compare these findings with the limited data in the literature obtained using other models, testing modes, strain magnitudes, and sample conditions.

Brain material properties in the past have been measured in vitro during compression, shear and oscillatory loading [7-17]. The reported properties vary as much as an order of magnitude. The broad range of testing methods (large range of strain rates and magnitudes, different species, locations, specimen preparations, and testing modes) along with the nonlinearity of brain tissue makes comparisons difficult. We tested a continuum of strains within a single sample to overcome the difficulty of comparing small strain and finite strain properties across different samples or tests. The results of experiments at higher strain rates show that this hyperelastic model for brain tissue is valid for a large range of strain rates (up to 16.7 s^{-1}). In addition, the nonlinearity of the samples could be modeled for both testing protocols employed.

To overcome difficulty with comparing material representations of brain tissue developed for different testing modes, we employed unconfined compression tests to validate the material model in a different mode of deformation. The compression results were in excellent agreement with the predicted response using the material parameters found from the simple shear tests (Figure 9), showing the Ogden hyperelastic material model can be used to accurately represent brain tissue material properties. However, our long-term stress relaxation behavior to an applied step displacement in unconfined compression tests is approximately ten times more compliant than material properties found by Mendis et al. and Miller et al. [12, 13]. The stiffer properties reported in the literature may be attributable to no-slip boundary conditions, lack of preconditioning of the samples, or postmortem storage conditions.

The properties determined in this paper for adult brain tissue correlate most closely with previous large deformation simple shear studies performed by Donnelly and Medige [9]. We used the nonlinear viscoelastic model determined by Donnelly and Medige for a constant rate displacement in simple shear and compared the results with our data. The nonlinear nature of this model fit our data well at 5% and 50% but the properties in the literature were approximately 4.25 times stiffer at both strains than those obtained in the present study. These material properties reported previously may be stiffer because they were determined from experiments conducted at least 12 hours postmortem, as well as using different strain rates and specimen locations than those used in the present study.

Due to the difficulty in obtaining human brain samples, porcine tissue is often used as a substitute for brain material testing [8, 13, 17, 19]. However, other laboratories have tested human tissue obtained at autopsy to avoid potential phylogenic differences in the properties [9, 10, 16, 24]. The advantage of using porcine brain tissue is that it is easily procured and can be tested shortly after death, therefore reducing the effects of the tissue degradation on the mechanical properties. We examined the relative difference between porcine tissue and a limited series of fresh human material to determine if any significant species differences existed in the mechanical behavior. To our knowledge, the human surgical sample data in this paper were obtained at much earlier time points after excision than previous studies, and are the only fresh, non-autopsy human data available. These human temporal lobe gray matter samples (n=5) were compared to the porcine gray matter samples and were found to be stiffer (29%) at every time point (Figure 4). The human specimens were obtained from temporal lobectomies performed on epilepsy patients. Therefore, we cannot rule out the possibility that the difference between the human and porcine tissue properties may be attributable to the abnormal human samples. Of note, though, is that these fresh human tissue properties are considerably less stiff than the human autopsy data in the literature, placing it far closer to fresh porcine data tested at large strain than human autopsy data.

Previous studies have investigated regional inhomogeneity in the brain, but they were limited to small oscillatory strains, and the results were reported using linear viscoelastic material models. Specifically, properties of the cerebrum [17] and brainstem [7, 25] were studied in shear, and the corona radiata and thalamic gray matter in torsion [16]. To compare the current data to these previous reports, only our small strain data (2.5%, combining directions 1 and 2) were fit to a standard linear model. All three regions were significantly less stiff than the brainstem [25]. Furthermore, the small strain moduli in the three regions were indistinguishable ($p=0.97$) from those reported for mixed gray/white matter porcine cerebral samples [17]. In contrast to our large strain findings, when only small strain data were considered there were no significant differences in the complex moduli between our three regions studied. Similarly, Shuck and Advani reported no significant differences in complex moduli between coronal radiata and gray matter at very low levels of strain (1.3%) and strain rates (<0.26s^{-1}) [16].

These distinctions between large and small strain behavior underscore the importance of characterizing the material behavior over the full range of distortions experienced during traumatic loads applied to the head. At large strains, when D1 and D2 data were combined, regional shear tests revealed significant differences between corona radiata, corpus callosum, and gray matter. Across time (t_i), gray matter was the stiffest region and corpus callosum the most compliant, with gray matter approximately 30% stiffer than corpus callosum. This regional inhomogeneity results in stress/strain concentrations that may play important roles in the regional tissue injury patterns reported in traumatic head injuries such as diffuse axonal injury and gliding contusions.

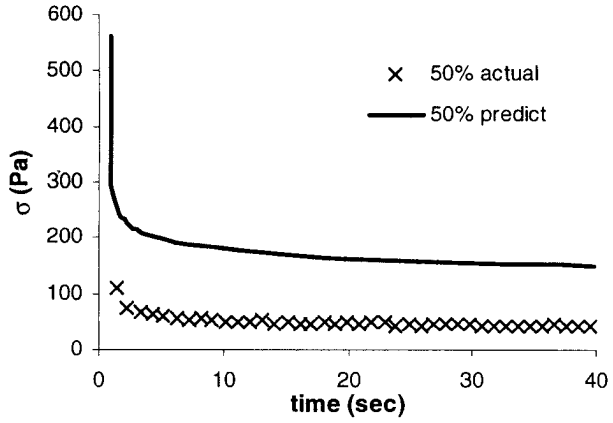

Figure 10: Prediction of linear Maxwell model

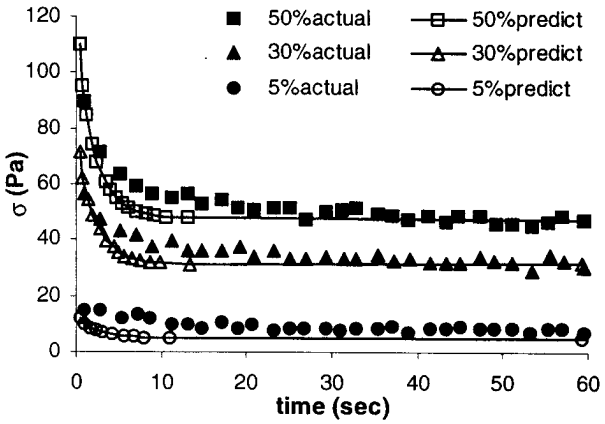

Figure 11: Prediction of Ogden hyperelastic model modified to include dissipation

In addition to regional inhomogeneity, our large strain shear tests demonstrate anisotropy, with the corpus callosum properties 1.93 times stiffer in D2 than D1. This finding is consistent with a uniaxial, fiber-reinforced model that we proposed previously for brainstem, with stiff viscoelastic fibers surrounded by a viscoelastic matrix [19]. In contrast, corona radiata and gray matter samples revealed D1 properties greater than D2. Although the corpus callosum region studied has a highly oriented, uniaxial structure, the corona radiata region also includes fibers that extend perpendicular to the major axis. A high proportion of these off-axis fibers would result in an increase in D1 modulus and decrease in D2 modulus. In fact, we find that the D1 properties of the corona radiata are indeed stiffer than those of the corpus callosum and the D2 properties of the corona radiata are less stiff than corpus callosum. Thus, development and examination of a multi-axial composite model would be more suitable for the corona radiata.

The nonlinear material model developed in this report appears to be a more representative material model for brain tissue across a broad range of strains compared to a linear viscoelastic representation. Our small strain data (5%) was fit to a 5th order linear Maxwell model and LS-DYNA (Livermore Software Technology Corp., Livermore, CA) was used to predict the 50% strain response in simple shear. As seen in Figure 10, the Maxwell model overestimated the shear stress at 50% shear strain. A similar finite element simulation was performed using ABAQUS Explicit 5.7 (HKS Inc., Pawtucket, RI) using the Ogden hyperelastic model modified to include dissipation. This model accurately predicts the shear stress at the top face of the tissue at all strains ranging from 5% to 50% (Figure 11). The applicability of the Ogden material representation across a range of strains believed to encompass injury conditions [26-28], as well as its availability for use in commercial finite element packages, points to a new opportunity for modeling the response of the human head to impact using this improved material model. The dramatic difference in behavior between the linear and nonlinear representations at finite strains suggests that future modeling results for human head finite element models employing the modified Ogden formulation may show similar and important differences from those using linear or elastic descriptions.

Taken together, we find good agreement between our data obtained at small strains and those published previously in the literature for fresh brain tissue [8, 17, 25]. However, brain tissue is nonlinear, and its large strain behavior reveals some notable differences. In summary, we report significant inhomogeneity at large strains (up to 50%) between white and gray matter, and even between two white matter regions – corona radiata and corpus callosum. Specifically, we find average gray matter properties to be 1.3 times stiffer than the most compliant region, the corpus callosum. Second, we find significant anisotropy in all regions tested, with the degree of anisotropy correlated with local neuroarchitecture. Third, we demonstrate that a modified Ogden formulation is an effective material model for brain tissue undergoing large deformations in either shear or compression. Fourth, we find that fresh porcine and human brain tissues are approximately 4-10 times less stiff than previous reports in the literature for autopsy specimens. We propose that these large strain, regional and directional data should enhance the biofidelity of computational models and provide important information regarding the mechanisms of traumatic brain injury.

ACKNOWLEDGEMENTS

Funds were provided by the Center for Injury Prevention and Control at the Centers for Disease Control (R49/CCR-312712). The authors are grateful to Drs. A.C. Duhaime and G.H. Baltuch for their cooperation in providing surgical specimens, and John Noon for the design of the tissue indentor system.

REFERENCES

1. Lee, M., J. Melvin, and K. Ueno. *Finite element analysis of traumatic subdural hematoma.* in *31st Stapp Car Crash Conference.* 1987.
2. Margulies, S., L. Thibault, and T. Gennarelli, *Physical model simulations of brain injury in the primate.* Journal of Biomechanics, 1990. **23**(8): p. 823-836.
3. Meaney, D., et al., *Biomechanical analysis of experimental diffuse axonal injury.* Journal of Neurotrauma, 1995. **12**(4): p. 311-322.
4. Mendis, K., *Finite element modeling of the brain to establish diffuse axonal injury criteria.* 1992, Ohio State University.
5. Miller, R., et al. *Finite element modeling approaches for predicting injury in an experimental model of severe diffuse axonal injury.* in *Proceedings of 42nd Stapp Car Crash Conference.* 1998. Tempe, AZ: SAE.
6. Zhou, C., T. Khalil, and A. King. *A new model comparing impact responses of the homogeneous and inhomogeneous human brain.* in *39th Stapp Car Crash Conference.* 1995. San Diego, California.
7. Arbogast, K. and S. Margulies, *Material characterization of the brainstem from oscillatory shear tests.* Journal of Biomechanics, 1998. **31**: p. 801-807.
8. Brands, D., et al. *Comparison of the dynamic behaviour of brain tissue and two model materials.* in *Proceedings of 43rd Stapp Car Crash Conference.* 1999. San Diego: SAE.
9. Donnelly, B. and J. Medige, *Shear Properties of Human Brain Tissue.* Journal of Biomechanical Engineering, 1997. **119**: p. 423-432.
10. Fallenstein, G. and V. Hulce, *Dynamic mechanical properties of human brain tissue.* Journal of Biomechanics, 1969. **2**: p. 217-226.
11. Galford, J. and J. McElhaney, *A viscoelastic study of scalp, brain, and dura.* Journal of Biomechanics, 1970. **3**: p. 211-221.
12. Mendis, K., R. Stalnaker, and S. Advani, *A Constitutive Relationship for Large Deformation Finite Element Modeling of Brain Tissue.* Journal of Biomechanical Engineering, 1995. **117**: p. 279-285.
13. Miller, K. and K. Chunzei, *Constitutive modeling of brain tissue: Experiment and theory.* Journal of Biomechanics, 1997. **30**: p. 1115-1121.
14. Miller, K., *Constitutive model of brain tissue suitable for finite element analysis of surgical procedures.* Journal of Biomechanics, 1999. **32**: p. 531-537.
15. Prange, M., G. Kiralyfalvi, and S. Margulies. *Pediatric rotational inertial brain injury: the relative influence of brain size and mechanical properties.* in *43rd Stapp Car Crash Conference.* 1999: SAE.
16. Shuck, L. and S. Advani, *Rheological response of human brain tissue in shear.* Journal of Basic Engineering, 1972: p. 905-911.
17. Thibault, K. and S. Margulies, *Age-dependent material properties of the porcine cerebrum: effect on pediatric inertial head injury criteria.* Journal of Biomechanics, 1998. **31**: p. 1119-1126.
18. Pieropaoli, C. and P. Basser, *Toward a Quantitative Assessment of Diffusion Anisotropy.* Magnetic Resonance in Medicine, 1996. **36**: p. 893-906.
19. Arbogast, K. and S. Margulies, *A fiber-reinforced composite model of the viscoelastic behaviour of the brainstem in shear.* Journal of Biomechanics, 1999. **32**(7): p. 865-870.
20. *Mock cerebrospinal fluid (CSF): KCl 0.220g, MgCl 0.132g, CaCl2 0.221g, NaCl 7.71g, Urea 0.402g, Dextrose 0.665g, NaHCO3 2.066g, distilled water 1000mL.*
21. Arbogast, K., et al., *A high frequency shear device for testing soft biological tissues.* Journal of Biomechanics, 1997. **30**: p. 757-759.
22. Ogden, R., *Non-linear elastic deformations.* 1984, Chichester, England: Ellis Harwood Ltd. (reprinted by Dover Publications Inc, Mineola, New York, 1997).
23. McElhaney, J., V. Roberts, and J. Hilyard, *Handbook of Human Tolerance.* 1976, Tokyo: Japan Automobile Research Institute.
24. Estes, M. and J. McElhaney. *Response of brain tissue to compressive loading.* in *Fourth ASME Biomechanics Conference.* 1970.
25. Arbogast, K. and S. Margulies. *Regional differences in mechanical properties of the central nervous system.* in *Proceedings of 41st Stapp Car Crash Conference.* 1997: SAE.
26. Bain, A. and D. Meaney. *Thresholds for mechanical injury to the in vivo white matter.* in *43rd Stapp Car Crash Conference.* 1999: SAE.
27. Margulies, S. and L. Thibault, *A proposed tolerance criterion for diffuse axonal injury in man.* Journal of Biomechanics, 1992. **25**(8): p. 917-923.
28. Shrieber, D., A. Bain, and D. Meaney. *In vivo threshold for mechanical injury to the blood-brain barrier.* in *41st Stapp Car Crash Conference.* 1997: SAE.